



International Journal of Pharmaceuticals and Health care Research (IJPHR)

IJPHR | Vol.13 | Issue 2 | Apr - Jun -2025

www.ijphr.com

ISSN: 2306-6091

DOI : <https://doi.org/10.61096/ijphr.v13.iss2.2025.299-309>

Research

Formulation, Evaluation, and Optimization of Viloxazine-Loaded Chitosan Nanoparticles in In-Situ Gel for Nose-to-Brain Delivery in the Effective Management of Depression

Anshuman Mohanty¹, Abhinandan Danodia², Dibya lochan Mohanty³



¹JJTU Research Scholar, Department of Pharmacy, SJJTU, Rajasthan

²Department of Pharmacy, SJJTU, Rajasthan

³Department of Pharmaceutics, School of Pharmacy, Anurag University, Hyderabad

*Author for Correspondence: Anshuman Mohanty

Email: anshumanmohanty@outlook.com

	Abstract
Published on: 29 Jun 2025	<p>Depression is a debilitating mental health disorder that necessitates innovative drug delivery strategies for effective management. This study focuses on developing and optimizing viloxazine-loaded chitosan nanoparticles incorporated into an in-situ gel for nose-to-brain delivery to enhance therapeutic outcomes. VXCN-NPs were prepared using the ionic gelation method and optimized using a Box-Behnken statistical design. The optimized formulation demonstrated a mean particle size of 160 nm, entrapment efficiency of 70.1%, and a PDI of 0.4, ensuring uniformity and stability.</p> <p>The in-situ gel system exhibited optimal pH (5.58), viscosity (65.4 cps), and gelation temperature (31.4 °C), making it suitable for nasal administration. In-vitro release and ex-vivo permeation studies revealed sustained drug release and enhanced permeation through nasal mucosa, achieving an 82% cumulative drug permeation over 8 hours. Stability studies confirmed the formulation's robustness under standard storage conditions for three months.</p> <p>This novel VXCN-NPs in-situ gel system effectively bypasses the blood-brain barrier, enhancing drug bioavailability and minimizing systemic side effects, thereby presenting a promising platform for nose-to-brain delivery in the treatment of depression and other central nervous system disorders.</p>
Published by: DrSriram Publications	
2024 All rights reserved.  Creative Commons Attribution 4.0 International License.	
	Keywords: Depression, Viloxazine, Chitosan nanoparticles, Nose-to-brain delivery, In-situ gel, Central nervous system disorders

INTRODUCTION

Depression is a pervasive and debilitating mental health disorder that affects millions of individuals worldwide, significantly reducing their quality of life, productivity, and social functioning [1]. It manifests as a complex interplay of emotional, cognitive, and physiological symptoms, including persistent feelings of sadness, diminished interest or pleasure in activities, and disruptions in sleep, appetite, and concentration [2]. Despite the

availability of numerous pharmacological treatments, the efficacy of conventional oral antidepressants remains suboptimal due to inherent limitations such as poor bioavailability, delayed onset of therapeutic action, and a propensity for systemic side effects [3]. These shortcomings not only prolong patient suffering but also contribute to treatment non-adherence, highlighting the urgent need for innovative drug delivery systems [4]. Advanced approaches that enhance therapeutic precision, improve drug bioavailability, and minimize systemic exposure have the potential to transform the management of depression and improve overall patient outcomes [5].

Nose-to-brain drug delivery has emerged as a promising approach for targeting the central nervous system (CNS) more effectively, providing a groundbreaking alternative to conventional methods of drug administration [6]. This non-invasive route bypasses the blood-brain barrier (BBB), which often limits the delivery of therapeutic agents to the brain, by utilizing the olfactory and trigeminal nerve pathways to achieve direct transport [7]. This targeted delivery not only significantly enhances drug bioavailability but also reduces systemic exposure, thereby minimizing the likelihood of adverse effects and improving overall therapeutic efficacy [8]. Moreover, the rapid onset of action associated with intranasal delivery makes it particularly advantageous for treating CNS disorders that require immediate intervention [9].

Viloxazine, a norepinephrine reuptake inhibitor approved for the treatment of attention-deficit/hyperactivity disorder (ADHD) and depression, has demonstrated considerable promise in managing various central nervous system (CNS) disorders due to its unique pharmacological profile [10]. However, its widespread clinical application has been constrained by inherent challenges, including limited aqueous solubility, low bioavailability, and suboptimal therapeutic concentrations at the target site [11]. These barriers underscore the necessity for advanced drug delivery systems to maximize its therapeutic potential [12].

The encapsulation of viloxazine into nanoparticles represents a robust strategy to overcome these limitations. Nanoparticles provide a means to improve the solubility and stability of viloxazine while enabling controlled and sustained release, ensuring prolonged therapeutic efficacy [13]. Among various nanoparticle carriers, chitosan has garnered significant interest due to its exceptional properties, including biocompatibility, biodegradability, and inherent mucoadhesive characteristics [14]. These features not only enhance the residence time of the formulation at the site of administration but also facilitate increased permeability of the drug across biological membranes, particularly via the intranasal route [15].

Furthermore, chitosan-based nanoparticles align seamlessly with intranasal delivery systems, offering a dual advantage [16]. On one hand, they leverage the unique properties of the nasal mucosa to bypass the blood-brain barrier (BBB), ensuring efficient delivery of viloxazine directly to the CNS. On the other hand, they minimize systemic exposure, thereby reducing the risk of adverse effects and enhancing patient safety [17]. Together, these attributes position chitosan nanoparticles as a transformative platform for optimizing viloxazine's therapeutic outcomes in CNS disorders.

In this study, we aimed to develop and optimize viloxazine-loaded chitosan nanoparticles incorporated into an in-situ gel system for intranasal administration. The in-situ gel acts as a sustained-release matrix, improving drug retention at the site of absorption and further enhancing brain-targeting efficiency. The developed formulation was systematically evaluated for particle size, entrapment efficiency, PDI and drug release profile.

Material and Methods

Viloxazine was used as the active ingredient & were purchased from Medcent Pharma (Hyderabad, India). Chitosan used as biodegradable polymer and were purchased from BLD Pharmatech (Hyderabad India). Sodium tri poly phosphate, Glacial acetic acid, and Carbopol-934 were purchased from Research-Lab Fine Chem Industries (Mumbai, India). Poloxamers-407 was obtained from Yarro chem (Mumbai, India) and additionally Ethanol, DMSO, Acetone, Ether which are used as solvents were obtained from S.D. Fine Chemicals (Mumbai India). All the reagents and solvents were of analytical reagent (AR) grade.

Preparation of Viloxazine loaded chitosan nanoparticles (VXCN-NPs):

Ionic gelation was used to formulate chitosan nanoparticles [18]. 150 mg of chitosan was added to 100 mL of distilled water and left overnight. Separately, 0.5% acetic acid was prepared and slowly added to the chitosan solution while stirring constantly for 30 minutes. 10 mg of the drug and Sodium tri poly phosphate (TPP) solution (0.15% in 100 mL of water) were added to 25 mL of the chitosan solution, which was placed on a magnetic stirrer for two to three hours. The chitosan nanosuspension formulated was then centrifuged at 12,000 rpm to collect the supernatant, which was used to calculate the particle size range and encapsulation efficiency (EE%).

Experimental Design

VXCN-NPs was optimized by a three-factor and three-level (−1, 0, +1) Box–Behnken statistical design (BBD) (design expert software version 8.0.7.1) using three independent and three dependent factors. The Chitosan (0.2–0.4 w/w, X1), TPP (1.5–2.5% w/w, X2), and Stirring Speed (400–500rpm, X3) were chosen as independent parameters, and their influence was evaluated on dependent variables like particle size (PS), entrapment efficiency

(EE) and Polydispersity index (PDI). A total of 17 formulations in different compositions were obtained from the software (Table 1). All formulations were prepared and examined for PS, EE and PDI. The values of PS, EE and PDI of all VXCN-NPs formulations were put into software to analyze the different experimental models (linear, 2nd order, and quadratic). The statistical analysis was performed for different models, and the best-fit model was selected. Polynomial equations and response plots for each response were constructed for examination of the effect of ingredients on the responses.

Table 1: Box-Behnken design with all factors in different level for VXCN-NPs formulations

Independent Variables(X)	Coded Value		
	Low (-1)	Mid (0)	High (+1)
X1= Chitosan (% w/w)	0.2	0.3	0.4
X2= TPP (% w/w)	1.5	2	2.5
X3= Stirring speed (rpm)	400	450	500
Responses(Y)	Constraint		
Y1= Particle size(Y1)	Minimize		
Y2= Entrapment efficiency (Y2)	Maximize		
Y3= PDI (Y3)	<1		

Table 2: Composition of VXCN-NPs and data of PS, EE% and PDI

Formulation Code	Chitosan (X1)	TPP (X2)	Stirring speed(X3)	Particle size(nm)(Y1)	EE% (Y2)	PDI (Y3)
VXCN-NP1	0.3	2.5	500	157.5	88	0.213
VXCN-NP2	0.3	2	450	162.7	77.3	0.264
VXCN-NP3	0.2	2	500	156.6	80	0.269
VXCN-NP4	0.3	2	450	162.9	79.6	0.265
VXCN-NP5	0.4	0.1	450	160	91	0.199
VXCN-NP6	0.4	2	400	165.6	87	0.198
VXCN-NP7	0.3	0.1	400	157	77	0.315
VXCN-NP8	0.4	2.5	450	164.6	89	0.187
VXCN-NP9	0.3	2	450	162.8	81	0.265
VXCN-NP10	0.4	2	500	161.9	83	0.185
VXCN-NP11	0.2	2	400	159.9	73	0.314
VXCN-NP12	0.3	2	450	161.5	77	0.249
VXCN-NP13	0.3	2.5	400	165.1	80.5	0.258
VXCN-NP14	0.2	2.5	450	155	88	0.261
VXCN-NP15	0.3	0.1	500	159.3	73	0.263
VXCN-NP16	0.3	2	450	162.7	76	0.262
VXCN-NP17	0.2	0.1	450	157.1	67	0.314

Characterization of VXCN-NPs

Particle Size Analysis and PDI Measurements

Zeta-size analysis was used to measure the PDI and particle size of VXCN-NPs. At 25 °C, the size was ascertained by dispersing NPs in distilled water at a concentration of 200 µg/mL. Nozzle potential (NP) electrophoretic velocities were measured using an electric field of 150 mV. Three independent analyses were performed on each sample.

Entrapment efficiency (%EE)

To determine the entrapment efficiency (EE) of Viloxazine in NPs, the non-encapsulated medicine was extracted from the NPs using centrifugation at 15,000 rpm for 40 minutes (C-2). The drug concentration of the clear supernatant was ascertained by measuring absorbance using a UV-visible spectrophotometer. UV spectrophotometer at 272nm. Every sample was measured three times in duplicate. The fraction of EE is calculated by using following equation:

$$EE\% = \frac{\text{Total amount of drug added} - \text{Free drug in Supernatant}}{\text{Total Amount of drug added}} \times 100$$

FE-SEM

The NPs' surface morphology and form were studied with FESEM (4300 S). Coatings of NPs with a 200-500 °Å thickness were applied using a gold sputter module in an argon environment and high vacuum evaporator for SEM inspection. In preparation for the examination, the specimens were air-dried and subjected to a range of accelerating voltages at scanning.

FTIR

Fourier Transform Infrared Radiation (FTIR) spectrum measurements were performed at room temperature using an IR spectrophotometer. To assess the peak pattern and create comparisons, they were qualitatively completed. By forming a KBr disc, pure drug and Optimized formulation FTIR spectra were acquired, and the 400–4000 cm⁻¹ range was analyzed to look for any noteworthy interactions.

Structural Analysis by TEM

The optimized nanoparticles' topology, structural form, and surface morphology were all investigated using transmission electron microscopy (TEM). For TEM investigation, one drop of the well-dispersed optimum nanoparticle formulation (2 mg/mL) in water was put to a 300 mesh carbon-coated copper grid. After two minutes, the grid was allowed to air dry, tapped with filter paper to remove any remaining surface water, and then negatively stained with 2% phosphor tungstic acid for thirty seconds. The grid was let to air dry at room temperature before measurement. Images were taken at different magnifications using a transmission electron microscope and an 80kv accelerating voltage.

Differential Scanning Calorimetry (DSC)

The DSC thermograms of Viloxazine, chitosan, TPP, blank, and VXCN-NPs using a DSC Q2000 Instrument. After being weighed into T zero aluminium pans and covered with T zero lids, each sample was examined at a 10°C/min scan rate within the 30 to 350°C temperature range. The samples were conducted under a nitrogen stream of 50 mL/min while utilizing an empty reference pan.

Preparation of VXCN-NPs In-Situ Gel

The in-situ gel containing VXCN-NPs (equivalent to 0.8% w/w Viloxazine) was prepared using the cold method. To prepare the plain gel, Carbopol 934 (8%) was dispersed in water and kept overnight. Then the Carbopol 934 solution was neutralized by triethanolamine. To prepare Opt-VXCN-NPs gel, Opt-VXCN-NPs dispersion 10ml was mixed with 5 g plain gel under propeller homogenizer at 400 rpm until a homogeneous dispersion was achieved. The mixtures were then refrigerated overnight to ensure complete polymer swelling and uniform gel formation.

Evaluation of VXCN-NPs In-Situ Gel**Clarity**

On a black and white backdrop to evaluate the clarity of each formulation.

Gelling temperature

Gelling temperature is defined as the temperature at which a liquid phase transitions into a gel phase. To determine this, a test tube containing a 2 mL aliquot of the gel was submerged in a water bath. The temperature of the water bath was increased incrementally by 1°C, with a 5-minute equilibration period at each temperature. Gelation was identified when the meniscus ceased to move upon tilting the test tube to a 90° angle.

pH and viscosity of in situ gel

After adding 1 mL of the gel formulation to a 10 mL volumetric flask, the volume was diluted with 10 mL using pure water. To determine the pH of the finished solution, a digital pH meter was utilized. The viscosity of the in-situ gel was measured using a Brookfield viscometer DV-II+Pro with an S-94 spindle set to 100 rpm and 4 ± 1 °C.

Drug content

Using 10 mL of pH 5.5 phosphate buffer, 1 mL of VXCN-NPs in-situ gel was extracted by vortexing. Further dilutions were made using phosphate buffer pH 5.5 and monitored at 272 nm with a UV spectrophotometer.

Gel strength

Gel strength was evaluated by gelling 50 g of the formulation at 37 °C in a 100 mL graduated cylinder using a thermostat. A 35 g weight was placed on the gelled VXCN-NPs in-situ gel. The time required for the weight to sink 5 cm into the gel was recorded.

In-Vitro Release Studies:

The dialysis membrane was used to study the optimized formulation in vitro. 1 mL of formulation, 1 gram of Viloxazine Dispersion and VXCN-NPs in-situ gel (containing an equivalent amount of 4 mg Viloxazine) were disseminated in pH 5.5 PBS as a release medium in a dialysis membrane. The 300 mL release medium in a beaker was lowered into the sac.(54) The beaker was kept in a shaking incubator set at 37 °C with moderate agitation (400–450 rpm). Maintaining the sink's condition. At predetermined times, 5 mL of the release media were removed from each sample and replaced with the same medium. UV spectroscopy set at 272 nm was used to determine the drug content of the samples. The in vitro release data was also fitted to many common kinetics models; the model that best fit the data was indicated by the regression coefficient (R²) for each model.

Ex-vivo permeation studies on nasal mucosa:

Examination of medication permeability in vitro Freshly excised goat nasal mucosa was procured from the adjacent abattoir and immediately submerged in PBS pH 5.5. The tissue in the donor and receptor compartments was stabilized with PBS pH 5.5 before being stirred with a magnetic stirrer for fifteen minutes. The excised superior nasal membrane was then placed on a Franz diffusion cell. After 15 minutes, the solution from both compartments was withdrawn, and fresh PBS with a pH of 5.5 was added to the receptor compartment. The temperature of the receiver chamber, which held 8 ml of diffusion medium, was kept at 37±2° C with continuous swirling at 400 rpm so that the nasal membrane's surface was hardly in contact with the diffusion fluid. Either VXCN-NPs in-situ gel or 2 mg/ml of Viloxazine Dispersion were stored in the donor compartment. Samples from hours 0, 1, 2, 3, 5, 6, and 7 were removed from the receptor compartment and replaced with 1mL of PBS pH 5.5. The samples were analyzed using a UV-Visible Spectrophotometer at 272 nm.

Stability Studies

The optimized VXCN-NPG4 was subjected to stability assessment by storing it in a room for three months at standard conditions according to ICH. NPs were placed in a 5 mL dark vial with a cap. In addition, samples were obtained at the start and end of the three months to determine the physical appearance, particle size, % entrapment efficiency and PDI.

Results and Discussion

Optimization and Statistical Analysis

Effect of independent factors on particle size (Y1)

The least-square second-order polynomial equation for particle size obtained from BBD (after ignoring insignificant factors) at 95% confidence.

$$PS(Y1) = 162.52 + 3.33X1 + 15.15B + 3.19C - 8.42AB - 1.25AC + 4.38BC - 0.7333A^2 - 13.36B^2 + 6.82C^2$$

Based on the results obtained from ANOVA (Table xx) for the BBD, F-value of the optimized model (obtained after omitting the in significant terms in the model) for particle size was found to be significant (F-value= 13.28, Pcal<0.0001), while the lack-of-fit was found to be insignificant (F-value = 12.95, Pcal = 0.0836) implying that model is significant. A three-dimensional surface map of the impacts of the independent variables (Chitosan, TPP, and Stirring speed) on particle size is presented in Figure 1(a, b, and c).

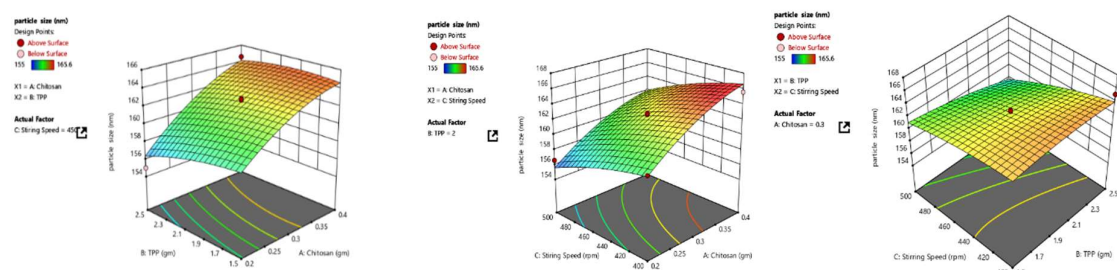


Fig 1: Response 3D surface plots for the (a) effect of Chitosan and TPP, (b) Effect of Chitosan and Stirring speed, (c) Effect of TPP and Stirring speed on particle size.

Effect of independent factors on Entrapment Efficiency % (Y2)

The least-square second-order polynomial equation for particle size obtained from BBD (after ignoring insignificant factors) at 95% confidence

$$PS(Y1) = 162.52 + 3.33X1 + 15.15B + 3.19C - 8.42AB - 1.25AC + 4.38BC - 0.7333A^2 - 13.36B^2 + 6.82C^2$$

Based on the results obtained from ANOVA for the BBD, F-value of the optimized model (obtained after omitting the in significant terms in the model) for particle size was found to be significant (F-value= 13.28, Pcal<0.0001),

while the lack-of-fit was found to be insignificant (F-value = 12.95, Pcal = 0.0836) implying that model is significant.

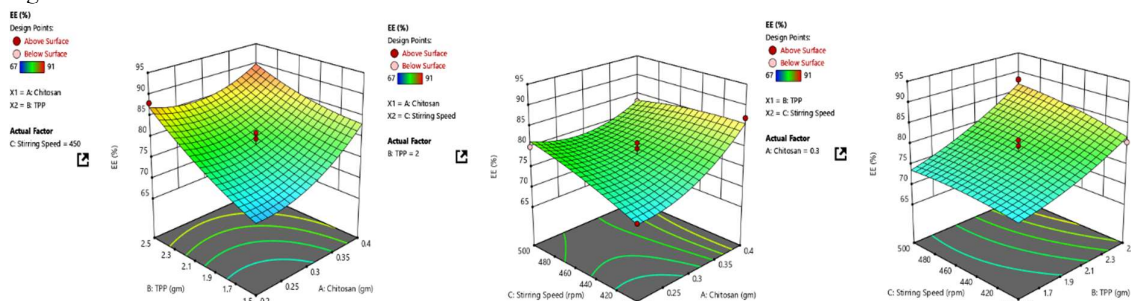


Fig 2: Response 3D surface plots for the (a) effect of Chitosan and TPP, (b) Effect of Chitosan and Stirring speed, (c) Effect of TPP and Stirring speed on EE%

Effect of independent factors on PDI (Y3)

The least-square second-order polynomial equation for particle size obtained from BBD (after ignoring insignificant factors) at 95% confidence

$$PS(Y1) = 162.52 + 3.33X1 + 15.15B + 3.19C - 8.42AB - 1.25AC + 4.38BC - 0.7333A^2 - 13.36B^2 + 6.82C^2$$

Based on the results obtained from ANOVA (Table xx) for the BBD, F-value of the optimized model (obtained after omitting the insignificant terms in the model) for particle size was found to be significant (F-value = 13.28, Pcal < 0.0001), while the lack-of-fit was found to be insignificant (F-value = 12.95, Pcal = 0.0836) implying that model is significant.

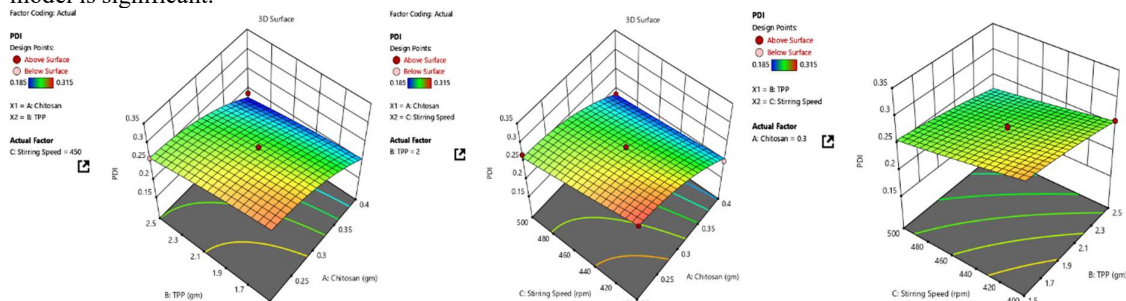


Fig 3: Response 3D surface plots for the (a) effect of Chitosan and TPP, (b) Effect of Chitosan and Stirring speed, (c) Effect of TPP and Stirring speed on PDI

Point prediction optimization

Optimized formulation was selected from point prediction of Box-Behnken software. Having 0.25% of Chitosan, 1.5% of TPP and 426.34 rpm stirring speed was found to full of our target goal and selected as an optimized formulation (**Opt-VXCN-NPs**). Optimized formulation was prepared and found to be PS of 160nm nm, EE of 70.1 %, and PDI 0.4 respectively. The **Opt-VXCN-NPs** formulation showed 100.46%, 100.1% and 101.31% of prediction of predicted value of responses (Y1, Y2, and Y3).

Table 3: Point of Prediction

Response Variable	Predicted values	Observed values	% Bias
Particle size(nm)	161.93	160	0.46
Entrapment Efficiency (%)	71.32	70.1	1.29
PDI	0.42	0.4	0.34

Particle size distribution and PDI of Opt-VXCN-NPs

The optimized Opt-VXCN-NPs has a mean particle size of 160 nm (Fig. 5a). The uniform size distribution and particle aggregation can both be well-indicated by the PDI. The typical range for PDI is 0.1 to 0.5. Higher PDI values signify a highly poly dispersed particle size distribution [19], while lower values imply samples that are predominantly monodispersed. For the optimised formulation, the PDI value is 0.4.

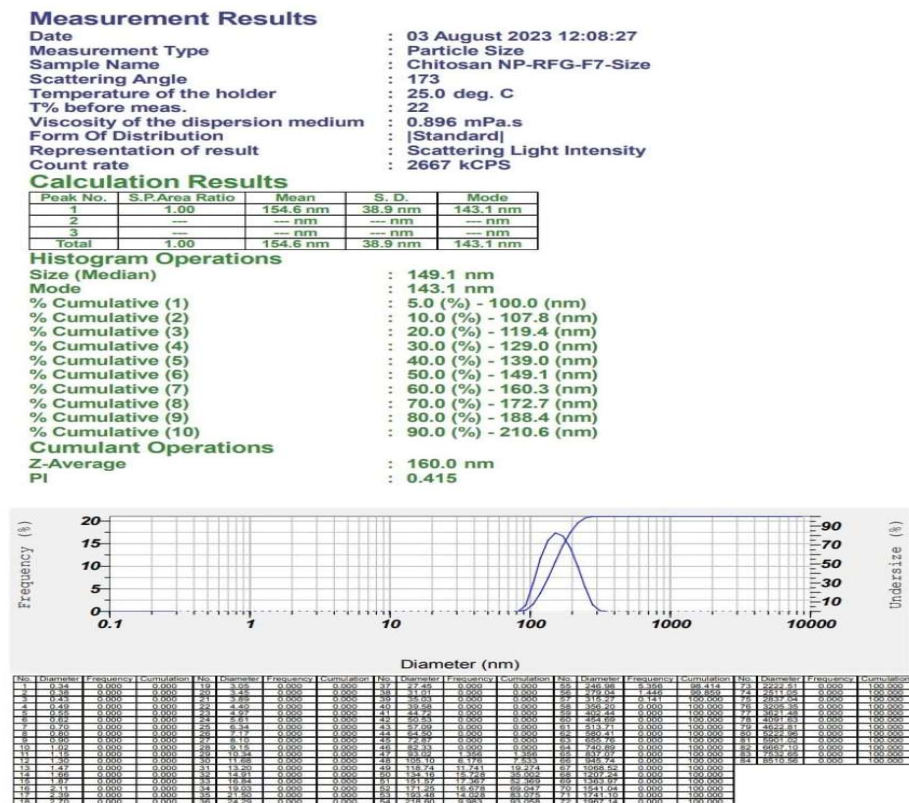


Fig 4: Particle size distribution and PDI of Opt-VXCN-NPs

SEM Study of Opt-VXCN-NPs

The micrographs also show that the particles are distributed well without any significant agglomeration. The optimized Opt-VXCN-NPs as observed under SEM are shown in Figure 5. The SEM image also confirmed the nano size and circular shape of the NP. The particle size of Chitosan NP s as observed with SEM was found to be in the nano range which corroborated with the size range obtained by photon correlation spectroscopy.

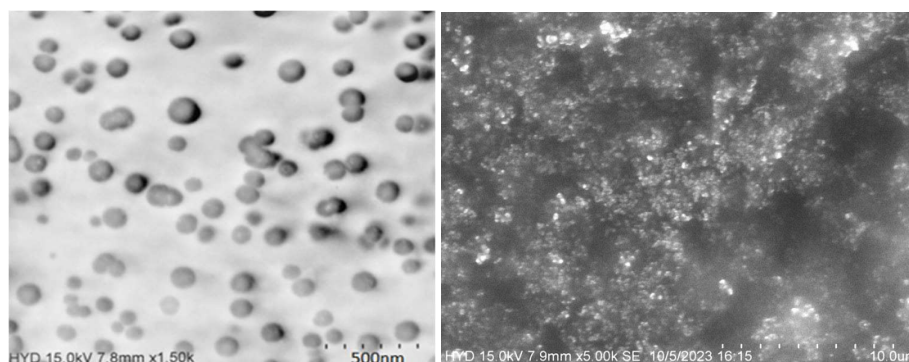


Fig 5: Scanning Electron Microscopy images of Opt-VXCN-NPs

DSC Study

Differential scanning calorimetry is used to detect changes in the drug's crystallinity and to identify any interactions between the drug and the excipients. It calculates the changes in enthalpy that result from endothermic or exothermic processes. 5 to 15 mg of drug samples were taken for analysis in standard aluminium pans. The empty pan is used as a guide. Mostly nitrogen is heated at this pace. Which served as a purge gas and liquid nitrogen was utilised to cool the system. The observed peak is 188°C as shown in the Figure 6.

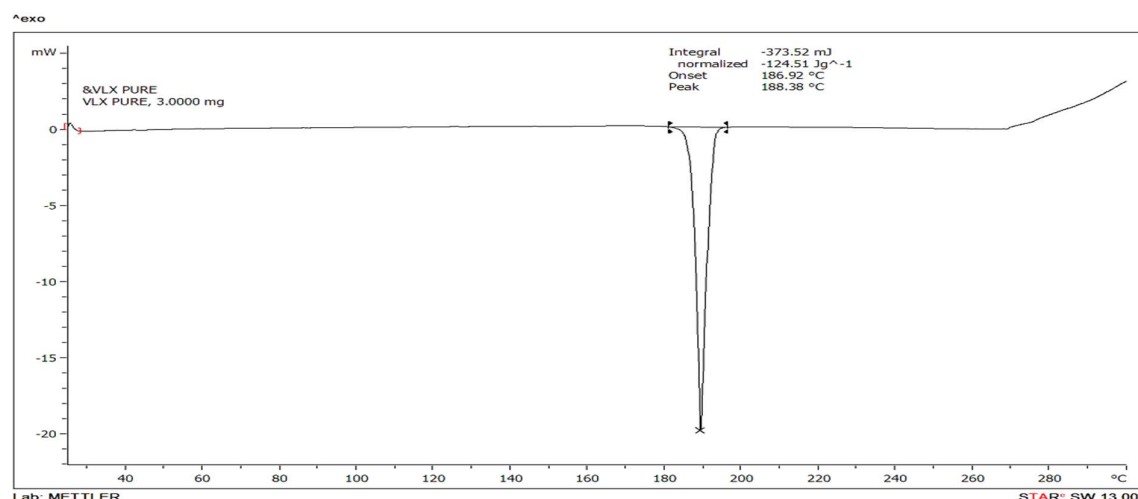


Fig 6: DSC of pure drug

Preparation of VXCN-NPs In-Situ Gel

To prepare the plain gel, Carbopol 934 (8%) was dispersed in water and kept overnight. Then the Carbopol 934 solution was neutralized by triethanolamine. To prepare **Opt-VXCN-NPs** gel, **Opt-VXCN-NPs** dispersion 10 mL was mixed with 5 g plain gel under propeller homogenizer at 400 rpm. To prepare conventional Viloxazine gel, Viloxazine solution was mixed with 5 g plain gel under propeller homogenizer at 400 rpm

Table 4: Formulation table for VXCN-NPs gel

Ingredient	VXCN-NPG1	VXCN-NPG2	VXCN-NPG3	VXCN-NPG4	VXCN-NPG5
Opt-VXCN-NP dispersion(ml)	10	10	10	10	10
Carbopol gel(gm)	1	1.5	2	2.5	5
Triethanolamine(ml)	1	1.5	1	1.5	2

Characterization of VXCN-NPs In-Situ Gel

Gels Clarity

Following evaluation, all formulations demonstrated clarity (Table 5). Notably, none of the formulations exhibited residual components that could potentially harm the nasal mucosa or compromise syringe ability.

pH and Viscosity

The pH of all VXCN-NPs in-situ gels was found to be 5.39 to 5.73 (Table 5), which revealed that it is compatible with nasal pH. The viscosity of all VXCN-NPs in-situ gel formulations was measured at 37 °C and found to be in the range of 33.4 cps (VXCN-NPG1) to 65.4 cps (VXCN-NPG4) (Table 5).

Gelling temperature

The gelling temperatures of the formulations ranged from 29.8 ± 0.1 to 36.6 ± 0.1 °C. Ideally, a gelling temperature between 25 and 37 °C is considered optimal. A gelling temperature below 25 °C may cause gel formation at room temperature. The mucoadhesive compound carbopol 934 similarly decreases the gelling temperature by promoting dehydration and enhancing the entanglement of adjacent molecules through more extensive intermolecular hydrogen bonding. The gelling temperature of the all-developed VXCN-NPs in-situ gels were measured, and the data are illustrated in Table 5.

Drug Content

The drug content of Viloxazine in all VXCN-NPs in-situ gels was found to be 80.14% to 94.75% (Table 5).

Table 5: VXCN-NPs In-Situ Gel Characterization

Formulation code	Clarity	pH	Gelling temperature	Viscosity (cps)	Drug content(%)	Gel strength
VXCN-NPG1	Clear	5.68	-	33.4	80.14	65.31

VXCN-NPG2	Clear	5.73	40.6	43.6	80.26	69.61
VXCN-NPG3	Clear	5.71	33.2	51.3	92.64	37.28
VXCN-NPG4	Clear	5.58	31.4	65.4	94.75	74.9
VXCN-NPG5	Clear	5.39	29.8	59.8	87.14	45.3

Ex-vivo Permeation Study

The drug permeation pattern through goat nasal mucosa reflected the release pattern as shown for in vitro release studies. The permeation of Viloxazine from VXCN-NPG4 gel through nasal mucosa was found to be more when compared with that of Viloxazine Dispersion. The cumulative percentage of Viloxazine permeated from VXCN-NPG4 after 8 h was found to be 82 %, after triplicate determinations. Permeation profile is shown in Figure 7.

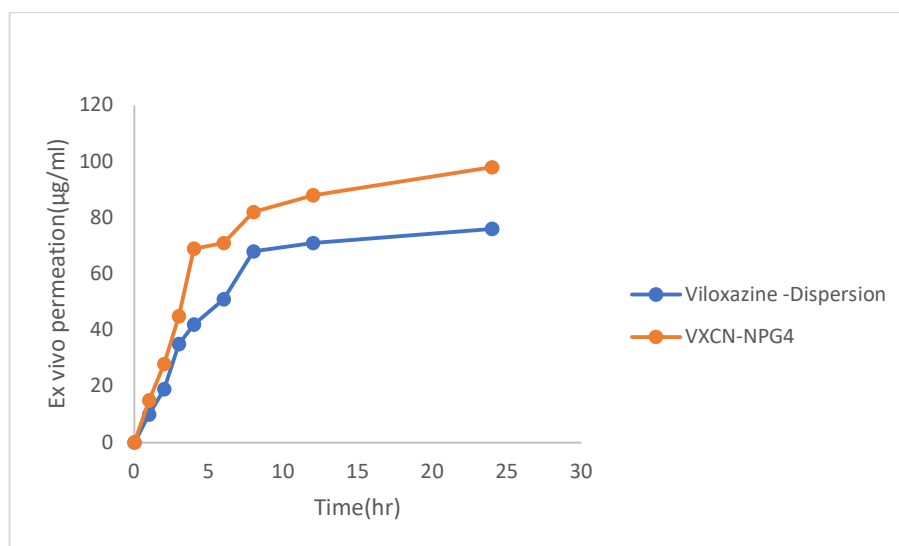


Fig 7: Ex-vivo Permeation graph

Stability studies

Stability studies of optimized batch of Viloxazine loaded chitosan nanoparticles gel (VXCN-NPG4) was carried out and stability of formulation was evaluated on the basis of physical appearance, particle size, entrapment efficiency and PDI as main parameters (Kalaria et al., 2009). The Viloxazine loaded chitosan nanoparticles gel did not show any change in visual appearance. Stability studies of optimized batch of Viloxazine loaded chitosan nanoparticles gel (VXCN-NPG4) was carried out and stability of formulation was evaluated on the basis of physical appearance, particle size, entrapment efficiency and PDI as main parameters it can be concluded that the Viloxazine loaded chitosan nanoparticles gel (VXCN-NPG4) is stable at $25 \pm 2^\circ\text{C}$ / $60 \pm 5\%$ RH for a total period of 3 months (Table 5).

Table 5: Stability study data of VXCN-NPG4

Stability parameter	Test Period			
	0 month	1 month	2 months	3 months
Particle size (nm)	160	160.1	161.9	162
EE%	70.1	70	68	67
PDI	0.4	0.4	0.3	0.3

CONCLUSION

This study successfully developed and optimized viloxazine-loaded chitosan nanoparticles (VXCN-NPs) incorporated into an in-situ gel system for nose-to-brain delivery aimed at enhancing the management of depression. The optimized formulation (Opt-VXCN-NPs) demonstrated favorable physicochemical properties, including a mean particle size of 160 nm, high entrapment efficiency (70.1%), and a PDI of 0.4, ensuring uniform

particle distribution. Characterization studies confirmed the nanoscale morphology and stability of the formulation. The in-situ gel system exhibited optimal pH, viscosity, and gelation temperature, making it compatible with nasal administration.

In-vitro and ex-vivo studies highlighted sustained drug release and enhanced permeation of viloxazine through nasal mucosa compared to conventional dispersion, achieving targeted delivery to the brain. The stability studies further established the robustness of the formulation under standard storage conditions over three months.

This approach effectively addresses the limitations of conventional antidepressant therapies by bypassing the blood-brain barrier, enhancing drug bioavailability, and minimizing systemic side effects. The findings underscore the potential of VXCN-NPs in-situ gel as a promising and innovative platform for nose-to-brain drug delivery in the treatment of CNS disorders such as depression.

CONFLICT OF INTEREST

The authors declare that there is no conflict of interest.

REFERENCES

1. Sharma A, Patel R. Environmental Degradation and Its Societal Consequences: A Comprehensive Study on the Relationship with Depression. *Advances in Urban Resilience and Sustainable City Design*. 2023 Aug 8;15(8):14-30.
2. Ovsianikova Y, Pokhilko D, Kerdyvar V, Krasnokutsky M, Kosolapov O. Peculiarities of the impact of stress on physical and psychological health. *Multidisciplinary Science Journal*. 2024 May 7;6.
3. Burbach L, Brult-Phillips S, Nijdam MJ, McFarlane A, Vermetten E. Treatment of posttraumatic stress disorder: a state-of-the-art review. *Current Neuropharmacology*. 2024 Apr 1;22(4):557-635.
4. Baryakova TH, Pogostin BH, Langer R, McHugh KJ. Overcoming barriers to patient adherence: the case for developing innovative drug delivery systems. *Nature Reviews Drug Discovery*. 2023 May;22(5):387-409.
5. Sharma A, Alam MA, Kaur A, Sharma S, Yadav S. Psychopharmacological Treatment of Depression and Anxiety and their Different Drug Delivery Targets. *Current Psychiatry Research and Reviews Formerly: Current Psychiatry Reviews*. 2024 Nov 1;20(4):297-322.
6. Agosti E, Zeppieri M, Antonietti S, Battaglia L, Ius T, Gagliano C, Fontanella MM, Panciani PP. Navigating the Nose-to-Brain Route: A Systematic Review on Lipid-Based Nanocarriers for Central Nervous System Disorders. *Pharmaceutics*. 2024 Feb 27;16(3):329.
7. Butola M, Nainwal N. Non-Invasive Techniques of Nose to Brain Delivery Using Nanoparticulate Carriers: Hopes and Hurdles. *AAPS PharmSciTech*. 2024 Dec;25(8):1-32.
8. Singh I, Kumar S, Singh S, Wani MY. Overcoming resistance: Chitosan-modified liposomes as targeted drug carriers in the fight against multidrug resistant bacteria-a review. *International Journal of Biological Macromolecules*. 2024 Aug 23;135022.
9. Jeong SH, Jang JH, Lee YB. Drug delivery to the brain via the nasal route of administration: exploration of key targets and major consideration factors. *Journal of pharmaceutical investigation*. 2023 Jan;53(1):119-52.
10. Montano CB, Jackson WC, Vanacore D, Weisler R. Considerations when selecting an antidepressant: a narrative review for primary care providers treating adults with depression. *Postgraduate Medicine*. 2023 Jul 4;135(5):449-65.
11. Wu K, Kwon SH, Zhou X, Fuller C, Wang X, Vadgama J, Wu Y. Overcoming Challenges in Small-Molecule Drug Bioavailability: A Review of Key Factors and Approaches. *International Journal of Molecular Sciences*. 2024 Dec 6;25(23):13121.
12. Emeihe EV, Nwankwo EI, Ajegbile MD, Olaboye JA, Maha CC. Revolutionizing drug delivery systems: Nanotechnology-based approaches for targeted therapy. *International Journal of Life Science Research Archive*. 2024;7(1):40-58.
13. McInturff EL, France SP, Leverett CA, Flick AC, Lindsey EA, Berritt S, Carney DW, DeForest JC, Ding HX, Fink SJ, Gibson TS. Synthetic approaches to the new drugs approved during 2021. *Journal of Medicinal Chemistry*. 2023 Aug 1;66(15):10150-201.
14. Harugade A, Sherje AP, Pethe A. Chitosan: A review on properties, biological activities and recent progress in biomedical applications. *Reactive and Functional Polymers*. 2023 Oct 1;191:105634.
15. Jeong SH, Jang JH, Lee YB. Drug delivery to the brain via the nasal route of administration: exploration of key targets and major consideration factors. *Journal of pharmaceutical investigation*. 2023 Jan;53(1):119-52.

16. Yadav S, Singh A, Palei NN, Pathak P, Verma A, Yadav JP. Chitosan-Based Nanoformulations: Preclinical Investigations, Theranostic Advancements, and Clinical Trial Prospects for Targeting Diverse Pathologies. *AAPS PharmSciTech*. 2024 Nov 5;25(8):263.
17. Baryakova TH, Pogostin BH, Langer R, McHugh KJ. Overcoming barriers to patient adherence: the case for developing innovative drug delivery systems. *Nature Reviews Drug Discovery*. 2023 May;22(5):387-409.
18. Esquivel R, Juárez J, Almada M, Ibarra J, Valdez MA. Synthesis and characterization of new thiolated chitosan nanoparticles obtained by ionic gelation method. *International Journal of Polymer Science*. 2015;2015(1):502058.
19. Danaei MR, Dehghankhold M, Ataei S, Hasanzadeh Davarani F, Javanmard R, Dokhani A, Khorasani S, Mozafari MR. Impact of particle size and polydispersity index on the clinical applications of lipidic nanocarrier systems. *Pharmaceutics*. 2018 May 18;10(2):57.